Food Microbiology 102 (2022) 103905

Contents lists available at ScienceDirect

Food Microbiology

journal homepage: www.elsevier.com/locate/fm

Integrative multiomics analysis of the acid stress response of *Oenococcus oeni* mutants at different growth stages

Qiling Chen [a,b,1], Xiangke Yang [a,d,1], Qiang Meng [a], Lili Zhao [a], Yuxin Yuan [a], Wei Chi [a], Ling He [c], Kan Shi [a,e,*], Shuwen Liu [a,e,**]

[a] College of Enology, Northwest A&F University, Yangling, Shaanxi, China
[b] College of Food Science and Pharmacy, Xinjiang Agricultural University, Urumqi, Xinjiang, China
[c] College of Horticulture, Northwest A&F University, Yangling, Shaanxi, China
[d] Henan University of Animal Husbandry and Economy, Zhenzhou, Henan, China
[e] Ningxia Helan Mountain's East Foothill Wine Experiment and Demonstration Station of, Northwest A&F University, Yongning, Ningxia, 750104, China

ARTICLE INFO

Keywords:
Oenococcus oeni mutants
Acid stress response
Genomic
Transcriptomic
Metabolomic

ABSTRACT

Background: Acid stress is one of the most important environmental stresses that adversely affect the growth of lactic acid bacteria (LAB), such as *Oenococcus oeni* which was isolated from grape-berries and mainly used in wine fermentation. The aim of this paper is to comprehensively characterize the mechanisms of acid stress regulation in *O. oeni* and to provide a viable theoretical basis for breed and improvement of existing LAB.
Method: First, six *O. oeni* mutants with acid-sensitive (strains b2, a1, c2) and acid-tolerant (strains b1, a3, c1) phenotypes were screened from three wild-type *O. oeni*, and then their genome (sequencing), transcriptome and metabolome (LC-MS/MS) were examined.
Results: A total of 459 genes were identified with one or more intragenic single nucleotide polymorphisms (SNPs) in these mutants, and were extensively involved in metabolism and cellular functions with a high mutation rates in purine (46%) and pyrimidine (48%) metabolic pathways. There were 210 mutated genes that cause significant changes in expression levels. In addition, 446 differentially accumulated metabolites were detected, and they were consistently detected at relatively high levels in the acid-tolerant *O. oeni* mutant. The levels of intracellular differentially expressed genes and differential metabolites changed with increasing culture time.
Conclusion: The integrative pathways analysis showed that the intracellular response associated with acid regulation differed significantly between acid-sensitive and acid-tolerant *O. oeni* mutants, and also changed at different growth stages.

1. Introduction

Lactic acid bacteria (LAB) are closely related to humans, animals and plants, naturally occurring in the environment and widely used in various areas of life. They are widely distributed in nature, and the species of LAB are richly diverse in the world and have been widely used in different fields, like agriculture, industry, food and medicine (Garcia-Diez and Saraiva, 2021; Li and Ganzle, 2020; Virdis et al., 2021). They also are the ideal genetic material for biochemical, genetic, and molecular biological studies. *Oenococcus oeni* (*O. oeni*) is the species of LAB most frequently associated with malolactic fermentation (MLF) in wine (Davis et al., 1986; Guzzon et al., 2009; Renouf et al., 2008; Torriani et al., 2011; Versari et al., 1999; Vigentini et al., 2016). Invariably, harsh physicochemical wine conditions, including low pH, greatly inhibit the growth of *O. oeni* and affect MLF. Acid stresses (AS) have mixed influences on *O. oeni*. Some physiological and molecular changes contribute to a more stress-tolerant state of *O. oeni* such as decreased membrane fluidity (Tourdot-Marechal et al., 2000), activated H^+-ATPase activity (Fortier et al., 2003), accelerated malate and citrate utilization (Olguin et al., 2009). The tolerance of LAB to AS is regulated

* Corresponding author. College of Enology, Northwest A&F University, Yangling, Shaanxi, China.
** Corresponding author. College of Enology, Northwest A&F University, Yangling, Shaanxi, China.
E-mail addresses: s.kan@nwafu.edu.cn (K. Shi), liushuwen@nwafu.edu.cn (S. Liu).
[1] Qiling Chen and Xiangke Yang contributed equally to this work. The order of names was decided by discussion and mutual agreement between the two co-first authors.

https://doi.org/10.1016/j.fm.2021.103905
Received 28 April 2021; Received in revised form 13 September 2021; Accepted 15 September 2021
Available online 20 September 2021
0740-0020/© 2021 Elsevier Ltd. All rights reserved.

by multiple mechanisms, and the full range of mechanisms regulating AS response throughout the whole growth period still needs to be further explored.

In this paper, the integrated regulatory mechanisms of six *O. oeni* mutants from three wild-type strains in response to acidic environment were investigated by multiomics analysis, revealing a series of global behaviors of *O. oeni* throughout the growth period when subjected to high AS.

2. Methods

2.1. O. oeni mutants preparation

Three wild-type strains SX-1a, SX-1b and CS-1b were isolated from the Shaanxi Province, and SE-AFLP analysis showed that SX-1a and SX-1b belong to different subgroups (Jin et al., 2014), and CS-1b had excellent β-glucosidase activity. Also, compared with SX-1a and CS-1b, SX-1b showed poor tolerance to acid environment. Low-energy N^+ beam implantation (Ion Beam Bioengineering Facility (UIL.0.512, TNV, Russia)) of *O. oeni* was performed for mutant preparation: the strains were grown in ATB medium (pH 4.8, 26 °C, glucose 10 g/L, yeast extract 5 g/L, peptone 10 g/L, $MgSO_4{\cdot}7H_2O$ 0.2 g/L, $MnSO_4{\cdot}4H_2O$ 0.05 g/L, cysteine/HCl 0.5 g/L and tomato juice 250 mL/L) to reach the intermediate exponential phase, two mL of bacterial solution was harvested by centrifugation (8000 rpm, 10 min) and suspended in 0.02% sodium hyaluronate solution. The suspensions were settled in a sample disc and then placed into the target chamber of the Ion Beam Bioengineering Facility. When the vacuum in the target chamber was below 10^{-2} Pa, the strains in the sample tray were implanted with low energy (30 KeV) N^+ with ion fluences of 1×10^{15} N^+/cm^2, 2×10^{15} N^+/cm^2, 3×10^{15} N^+/cm^2, 4×10^{15} N^+/cm^2 and 5×10^{15} N^+/cm^2. The implanted strains were then cultured directly in stress ATB medium (pH 3.0/pH 9.0, adjusted by HCl/NaOH). The strains were revived and cultured continuously in the same stress medium for at least 20 generations. Then, a single colony was isolated with ATB agar medium (50 mg/L cycloheximide and 20 mg/L vancomycin) and sub-cultured in the same stress medium for 20 generations to obtain a heritable phenotype mutants of b1, a3, and c1 (from the wild-type strains SX-1b, SX-1a, and CS-1b, respectively, after stress cultivation at pH 3.0; defined as acid-tolerant mutants) and b2, a1, and c2 (from the wild-type strains SX-1b, SX-1a, and CS-1b, respectively, after stress cultivation at pH 9.0; defined as acid-sensitive mutants).

2.2. Genome sequencing and assembly

The mutants were cultured to exponential phase in ATB broth at 26 °C, pH 4.8, were collected and the genomic DNA was purified using the TIANamp Bacterial DNA Kit (TIANGEN BIOTECH, BEIJING). The genomes of six mutants were sequenced using massively parallel sequencing Illumina technology (Illumina HiSeq2500) and the paired-end read libraries were constructed with one insertion of 500 bp and one insertion of 5 kb, respectively. Next, Illumina PCR adapter reads and low-quality reads were filtered out. The filtered reads were assembled by SOAPdenovo (http://soap.genomics.org.cn/soapdenovo.html) to generate scaffolds. All reads were used for further gap closure.

2.3. Comparative genomics

MUMmer and LASTZ alignment tools were used to compare the complete genome sequences of different species for SNPs. Core/pan genes were clustered by the CD-HIT rapid clustering of similar proteins software with a threshold of 50% pairwise identity and 0.7 length difference cutoff in amino acids.

2.4. Total RNA extraction and Illumina sequencing

The mutants growing in pH 3.0 ATB medium were harvested at transition phase (3 h samples), exponential growth phase (36 h samples) and the stationary phase (108 h samples). Total RNA was extracted according to the TRIzol-based method (Life Technologies, CA, USA). The cDNA libraries from the mutants were sequenced using Illumina sequencing platform with paired-end 150-base reads by Genedenovo Biotechnology Co., Ltd (Guangzhou, China). Analysis was based on an independent library constructed by samples of all assays (all samples occupied triplicate parallel).

2.5. Identification of differentially expressed genes through RNA sequencing

The gene expression level was normalized by using the fragments per kilobase of transcript per million (FPKM) mapped reads method to offset the influence of different gene lengths and amounts of sequencing data on the calculation of gene expression. Differentially expressed genes (DEGs) were identified through the edgeR package (http://www.r-project.org/) with fold changes ≥2 (absolute Log_2FC (fold change) ≥ 1) with a false discovery rates-adjusted (FDRs) $P < 0.05$. Subsequently, DEGs were then subjected to Kyoto Encyclopedia of Genes and Genomes (KEGG) pathway enrichment analysis.

The threshold implies the p-value standardized to 0.05.

2.6. Coexpression network construction

Gene coexpression networks were created using the weighted gene coexpression network analysis (WGCNA) package in R.

2.7. Metabonomic extraction and analysis

One milliliter of precooled extractant (70% methanol aqueous solution, added 2- chlorophenylalanine as an internal standard) was added to the sample and vortexed for 1 min. Next, the samples were frozen directly in liquid nitrogen for 3 min, followed by thawing on ice for 3 min, vortexing for 2 min, and repeating this operation three times. Then, the samples were centrifuged at 12,000 rpm for 10 min at 4 °C to obtain the supernatant, which was bottled and analyzed by LC-MS/MS.

2.8. Chromatographic conditions

The chromatographic separations were performed on an HSS T3 (1.8 μm, 2.1 × 100 mm) column (Waters, Milford, MA) maintained at 40 °C through an LC-UPLC system (Shim-pack UFLC SHIMADZU CBM A). The mobile phase consisted of a linear gradient elution and was performed at 0.4 mL/min using 0.1% formic acid in water (mobile phase A) and in acetonitrile (mobile phase B). The gradient profile was from phase A to phase B 95: 5 (V/V) at 0 min, 10: 90 (V/V) at 11 min, 95: 5 (V/V) at 11.1–14 min.

2.9. ESI-Q TRAP-MS/MS

Triple quadrupole (QQQ) and LIT scans were acquired on a triple quadrupole-linear ion trap mass spectrometer (QTRAP), QTRAP® LC-MS/MS System, equipped with an ESI Turbo Ion-Spray interface, operating in positive and negative ion mode and controlled by Analyst 1.6.3 software (Sciex). The ESI source operation parameters were as follows: source temperature 500 °C; ion spray voltage (IS) 5500 V (positive), −4500 V (negative); ion source gas I (GSI), gas II (GSII), and curtain gas (CUR) were at 50, 50, and 25 psi, respectively; and the collision gas (CAD) was set at high. Instrument tuning and mass calibration were performed with 10 and 100 μmol/L polypropylene glycol solutions in QQQ and LIT modes, respectively. A specific set of MRM transitions was monitored for each period according to the metabolites eluted within

this period.

2.10. Screening of differential metabolites

Significantly regulated metabolites between groups were determined by VIP ≥1 and absolute $Log_2FC \geq 1$. VIP values were extracted from the OPLS-DA results, which also contained score plots and permutation plots, and were generated using the R package MetaboAnalystR. The data was log transformed (log_2) and mean centered before OPLS-DA. To avoid overfitting, a permutation test (200 permutations) was performed.

2.11. KEGG annotation and enrichment analysis

The identified metabolites were annotated using the KEGG compound database (http://www.kegg.jp/kegg/compound/), and annotated metabolites were then mapped to the KEGG Pathway database (http://www.kegg.jp/kegg/pathway.html). Pathways with significantly regulated metabolites mapped to were then fed into MSEA (metabolite sets enrichment analysis), and their significance was determined by hypergeometric distribution.

3. Results

3.1. The relationship between mutations and phenotypes

After 120 h of incubation at pH 3.0, *O. oeni* mutants b1, a3 and c1 (acid-tolerant mutants) showed maximum tolerance to pH 3.0 conditions in terms of growth trend, and the cell density of b1, a3, and c1 were significantly higher than those of the corresponding wild-type strains SX-1b, SX-1a and CS-1b. *O. oeni* mutants b2, a1 and c2 (acid-sensitive mutants) had the lowest cell densities when compared to the corresponding wild-type strains and acid-tolerant mutants (Fig. 1).

Whole-genome sequencing identified 1411 SNPs in 459 genes in six mutants (Table S1). Enrichment analysis revealed significant differences in the detection rates of these SNPs in purine metabolism, pyrimidine metabolism, fatty acid biosynthesis, fatty acid metabolism, drug metabolism, and metabolic pathways. Statistical analysis showed that the same loci for SNPs occurred within mutants of the same phenotype (acid-tolerant or acid-sensitive mutants), suggesting that SNPs were closely related to their phenotypes.

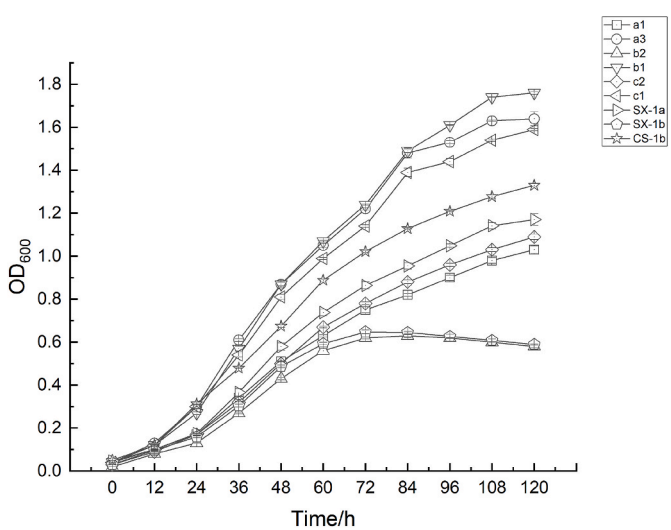

Fig. 1. Proliferative capacities of *O. oeni* mutants and corresponding wild-type strains cultivated with pH 3.0 ATB medium. The absorbance values (OD_{600} nm) were calculated as the tested samples' OD reading minus the negative control's OD reading. Error bars represent the SD of three biological repeats. Acid-tolerant mutants: b1, a3 and c1; acid-sensitive mutants: b2, a1 and c2, wild-type strains: SX-1a, SX-1b and CS-1b.

3.2. Analysis of transcriptome and metabolome of mutants

Transcriptome and metabolome analysis were performed for acid-tolerant mutant b1 and acid-sensitive mutant b2 at 3 h, 36 h and 108 h, respectively. These two mutants from the same wild-type strain presented the most pronounced phenotypic differences when incubated at pH 3.0 (Fig. 1).

For transcriptome, a total of 550 DEGs were detected by pairwise comparison of mutants (b1 vs b2) (Fig. 2A), of which 210 DEGs contained intragenic SNPs. The enrichment analysis of transcriptomic data (Fig. S1A-B) revealed that the ABC transporters and valine, leucine and isoleucine degradation pathways were significantly different between b1 and b2 in the 3 h and 36 h samples; phenylalanine, tyrosine and tryptophan biosynthesis in the 3 h samples; purine metabolism pathway in the 36 h samples; fatty acid biosynthesis, fatty acid metabolism and pyrimidine metabolism pathways in the 108 h samples. Then all the DEGs were subjected to WGCNA analysis, which is considered a more biologically and statistically significant method, and a bridge for the connection of sample traits and gene expression changes (Ai et al., 2020). And the results indicated that the DEGs in the blue module were most associated with acid tolerance-related traits (Figure S2).

Regarding metabolome, a total of 446 metabolites accumulated to different degrees at the three sampling points (b1 vs b2), and the number of up-regulated metabolites was higher than the number of down-regulated metabolites at all the sampling points (Fig. 2B). Pathway for arginine biosynthesis was significantly different between mutant b1 and mutant b2 in the 36 h and 108 h samples. Pathways for aminoacyl-tRNA biosynthesis, alanine, aspartate, glutamate, ABC transporter, galactose metabolisms were significantly different in the 3 h and 108 h samples. Pathways for glycine, serine, threonine, cysteine, methionine, glycerophospholipid, butanoate, thiamine, sulfur and nitrogen metabolisms were significantly different only in the 3 h samples (Fig. S3i-iii). The results showed that the response of *O. oeni* towards acid environment varied at different growth phase.

3.3. Integrated analysis of genomics, transcriptomics and metabolomics of mutants

Integration of multi-source data is crucial in enhancing AS response understanding and identifying meaningful clusters of molecular mechanisms. Therefore, we screened the integrated pathways (Table 1) of genomics, the blue module in WGCNA of transcriptomics and metabolomics associated with distinguishable phenotypic mutants to investigate how multiple alterations might jointly contribute to acid regulation in *O. oeni*.

3.3.1. Changes in pathways related to arginine and glutamate metabolism

In the arginine-glutamate-related metabolic pathways (Fig. 3, light green background), six genes, *arcA*, *pyrAA*, *carB*, *amiE*, *gabT* and *gabD*, were mutated (Table S2). Of them, *arcA* catalyzes the interconversion of arginine and citrulline accompanied by the emission of NH_3 (Budin-Verneuil et al., 2006; Cheng et al., 2013). The genes *pyrAA* and *carB* both encode carbamoyl phosphate synthase (Thoden et al., 2002), and the *gab* cluster (*gabT* and *gabD*) specifies the synthesis of the enzyme of the γ-aminobutyric acid (GABA) degradation pathway (Bartsch et al., 1990).

In b1, the relative expression of *arcA*, *gabT* were up-regulated in the 3 h samples, whereas *gabD* was down-regulated in the 3 h and 36 h samples, *pyrAA* and *carB* were down-regulated in the 3 h and 108 h samples, as compared to b2. The relative levels of arginine in b1 were consistently higher than that in b2 at all sampling points, and the relative levels of glutamate, glutamine and GABA in b1 were only higher in the 3 h samples (Table S3).

3.3.2. Changes in pathway related to aspartate metabolism

In the aspartate-related metabolic pathway (Fig. 3), genes required for the biosynthesis of pyrimidine and purine from aspartate, including

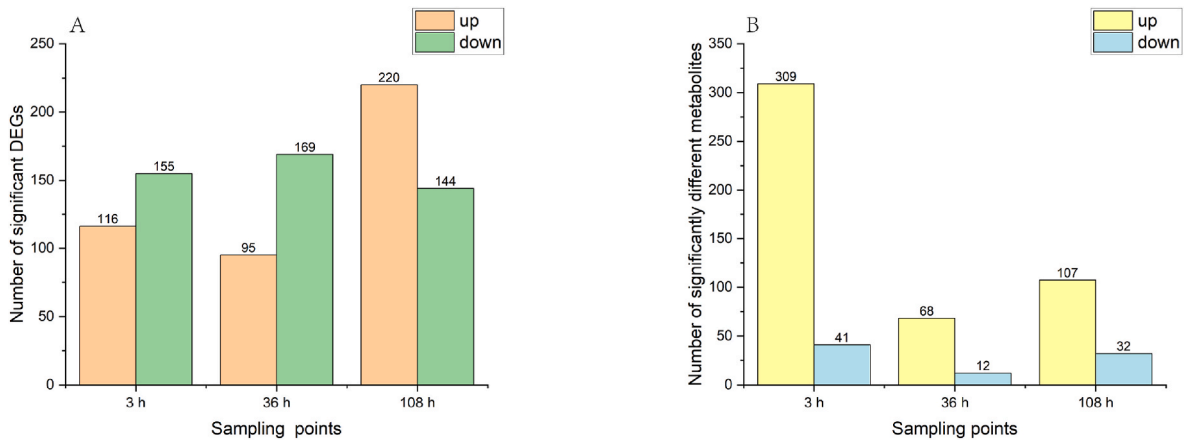

Fig. 2. The total number changes of DEGs (A) and differential metabolites (B) between b1 and b2 at different sampling points.

Table 1
Integrated KEGG enriched pathways based on multiomic analysis.

KEGG A class	KEGG B class	Pathways	Pathway ID
Metabolism	Amino acid	Arginine biosynthesis	ko00220
Metabolism	Amino acid	Alanine, aspartate and glutamate metabolism	ko00250
Metabolism	Amino acid	Glycine, serine and threonine metabolism	ko00260
Metabolism	Amino acid	Cysteine and methionine metabolism	ko00270
Metabolism	Amino acid	Valine, leucine and isoleucine degradation	ko00280
Metabolism	Amino acid	Lysine biosynthesis	ko00300
Metabolism	Amino acid	Arginine and proline metabolism	ko00330
Metabolism	Carbohydrate	Glycolysis/ Gluconeogenesis	ko00010
Metabolism	Carbohydrate	Pentose phosphate pathway	ko00030
Metabolism	Carbohydrate	Fructose and mannose metabolism	ko00051
Metabolism	Carbohydrate	Galactose metabolism	ko00052
Metabolism	Carbohydrate	Starch and sucrose metabolism	ko00500
Metabolism	Carbohydrate	Amino sugar and nucleotide sugar metabolism	ko00520
Metabolism	Carbohydrate	Pyruvate metabolism	ko00620
Metabolism	Carbohydrate	Butanoate metabolism	ko00650
Metabolism	Energy	Oxidative phosphorylation	ko00190
Metabolism	Energy	Sulfur metabolism	ko00920
Metabolism	Global and overview maps	Metabolic pathways	ko01100
Metabolism	Global and overview maps	Carbon metabolism	ko01200
Metabolism	Global and overview maps	Biosynthesis of amino acids	ko01230
Metabolism	Lipid	Glycerophospholipid metabolism	ko00564
Metabolism	Cofactors and vitamins	Nicotinate and nicotinamide metabolism	ko00760
Metabolism	Cofactors and vitamins	Folate biosynthesis	ko00790
Metabolism	Other amino acids	Glutathione metabolism	ko00480
Metabolism	Nucleotide metabolism	Purine metabolism	ko00230
Metabolism	Nucleotide metabolism	Pyrimidine metabolism	ko00240
Genetic information processing	Translation	Aminoacyl-tRNA biosynthesis	ko00970
Environmental information processing	Membrane transport	ABC transporters	ko02010

pyrB, *pyrD*, *pyrE*, and *pyrF*, were mutated (Burns et al., 1998; Murahari and West, 2019; Norager et al., 2003). Moreover, the *purA* and *purB* genes identified to catalyze the conversion of aspartate to fumarate (Tsai et al., 2007; Wang et al., 1997) were also mutated.

Among these genes, *pyrD* and *purA* were down-regulated at all sampling points, *pyrE* and *pyrF* were down-regulated at 36 h and 108 h (Table S2). Metabolomic data showed the relative level of aspartate in b1 was higher than that in b2 at 3 h (Table S3).

3.3.3. Changes in pathways related to cysteine and methionine metabolism

In the cysteine and methionine related metabolic pathways (Fig. 3, light blue background), gene *hom*encoding homoserine dehydrogenase, the third step enzyme involved in converting aspartate into methionine or threonine (Curien et al., 2005), was mutated. In addition, *metY* and *thrC*, the fifth step in the synthesis of methionine or threonine from aspartate, were mutated (Fig. 3 and Table S2). Among these genes, *metY* was down-regulated in the 36 h and 108 h samples, as well as *thrC* in the 3 h samples. Table S3 demonstrated relatively high levels of cysteine, homoserine, cystathionine and methionine in b1 at 3 h.

3.3.4. Changes in pathway related to glutathione metabolism

In the metabolic pathway of glutathione (Fig. 4), the *gor* gene (Ji et al., 2015; Sikanyika et al., 2019; Sugio et al., 1995), which encodes glutathione reductase, was mutated and the expression was up-regulated in the 108 h samples (Table S2). And the relative content of Glutathione (GSH) in b1 was only higher than that in b2 at 3 h (Fig. 4 and Table S3). This is consistent with the findings of Zhang et al. (2007), indicating that GSH can minimize the damage caused by short-term severe acid attack.

3.3.5. Changes in pathways related to carbohydrate metabolism

In the glycolysis pathway (Fig. 3, light orange background), the proteins encoded by mutated genes *tpiA* and *gapA* catalyze reversible reactions of glyceraldehyde-3P between glycerone-P and glycerate-1,3-bisphosphate (Schurig et al., 1995). Remarkably, the *fba* gene encoding fructose-bisphosphate aldolase in *O. oeni*, which is responsible for the reversible reaction between fructose-1,6-bisphosphate and glyceraldehyde-3P, was also mutated. Furthermore, in the pentose phosphate pathway, the gene *xfp* that catalyzes the conversion of xylulose-5P to glyceraldehyde-3P, was also mutated. However, no changes involving the above-mentioned genes had been detected in both transcriptomic and metabolomic data.

3.3.6. Changes in the pathway related to pyruvate metabolism

In the pyruvate metabolism pathway (Fig. 3, light purple background), *aceE* encoding pyruvate dehydrogenase E1 subunit alpha, exhibited 6 nonsyn sites. Furthermore, the mutated *poxL* and *pta* can

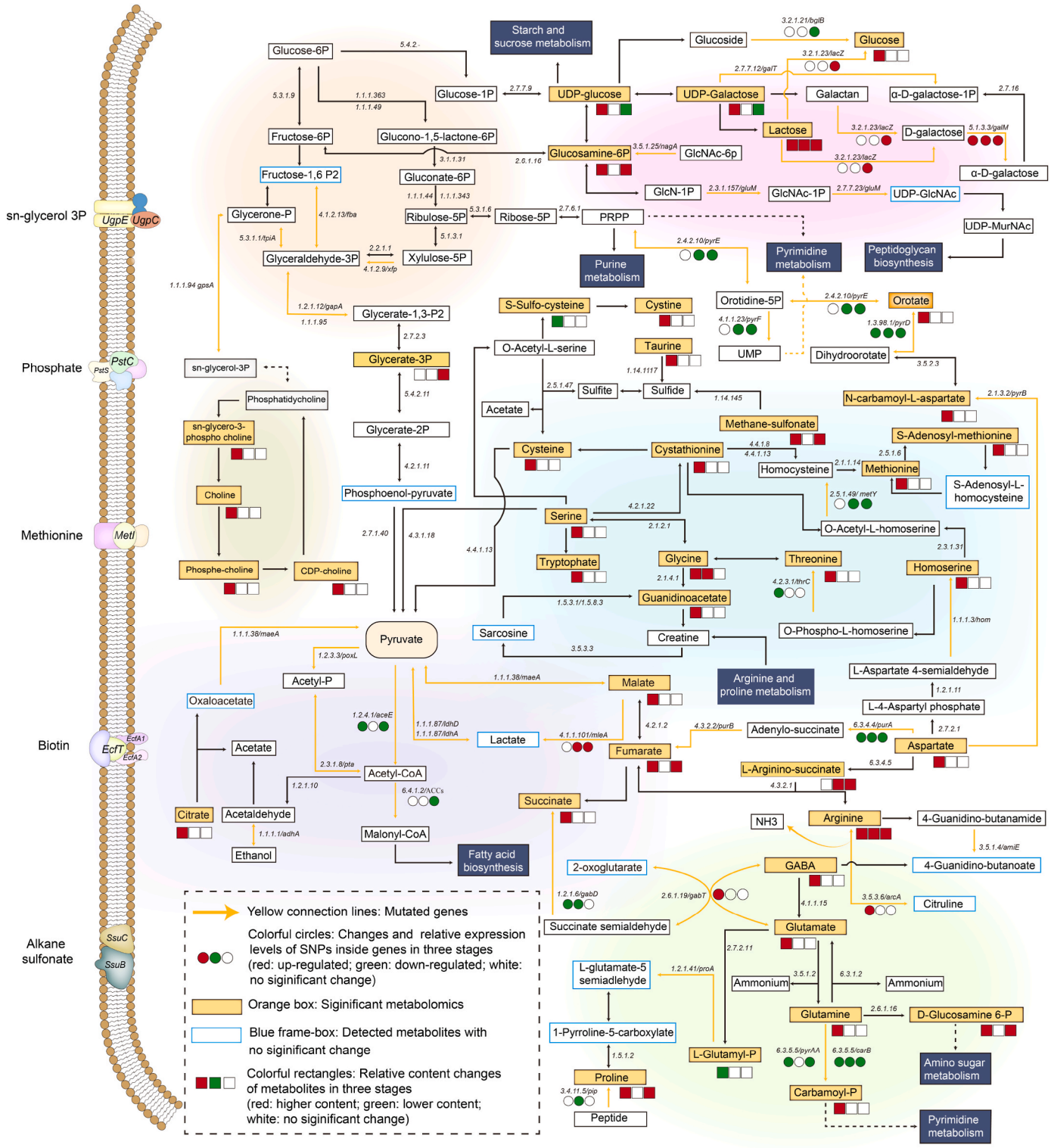

Fig. 3. Integrated pathways based on multiomic analysis of *O. oeni* acid regulation. Yellow connection lines represented the intragenic SNPs; the color circles represented the gene expression levels with intragenic SNPs (red, up-regulated; green, down-regulated; white, no significant change); the orange box indicated significant differences in metabolites between b1 and b2 mutants; blue frame box were the detected metabolites with no significant differences; color rectangles were the relative content changes of metabolites during the three growth stages (red, higher content; green, lower content; white, no significant change). (For interpretation of the references to color in this figure legend, the reader is referred to the Web version of this article.)

generate acetyl-CoA from pyruvate. Then the mutated genes *accA*, *accB* and *accD* (ACCs) encoding proteins catalyze the conversion of acetyl-CoA to malonyl-CoA (Bilder et al., 2006; Fries et al., 2003; Tian et al., 2005). The mutated *ldh* catalyzes the interconversion of pyruvate and lactate. Moreover, the mutated *maeA* encodes both malate dehydrogenase and oxaloacetate decarboxylase (Yamaguchi, 1979). The mutated gene *mleA* catalyzes malate into lactate. More importantly, the genes *maeA* and *mleA* are essential for *O. oeni* to utilize malate in oligotrophic

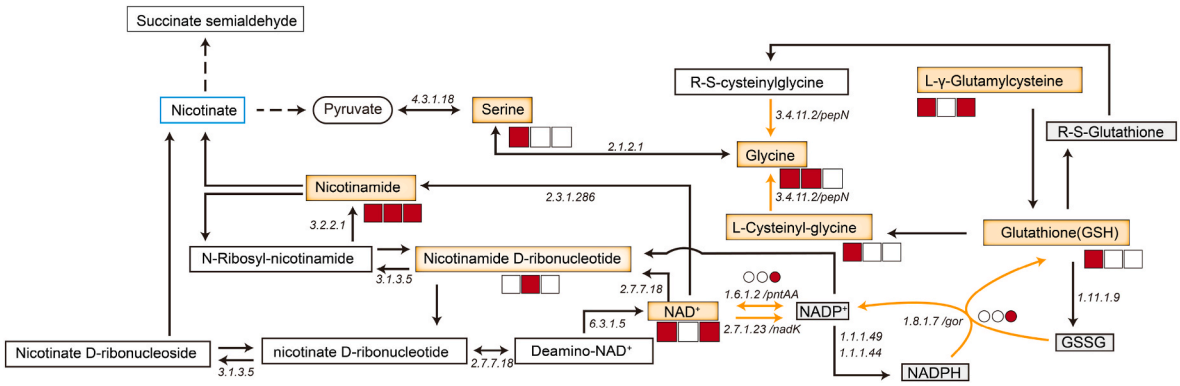

Fig. 4. Multiomics identified changes in the nicotinate, nicotinamide metabolism and glutathione metabolism pathways and the probable metabolic connection. Yellow connection lines represented the intragenic SNPs; the color circles represented the gene expression levels with intragenic SNPs (red, up-regulated; green, down-regulated; white, no significant change); the orange box indicated significant differences in metabolites between b1 and b2 mutants; blue frame box were the detected metabolites with no significant differences; color rectangles were the relative content changes of metabolites during three growth stages (red, higher content; green, lower content; white, no significant change). (For interpretation of the references to color in this figure legend, the reader is referred to the Web version of this article.)

environment after alcohol fermentation during vinification (Liu and Li, 2009).

Transcriptomic data showed the expressions of *aceE* was down-regulated in the 3 h and 108 h samples, ACCs were down-regulated in the 108 h samples, *ldh* was up-regulated in the 3 h samples, and gene *mleA* was up-regulated in the 36 h and 108 h samples (Table S2). Metabolomics data indicated that malate, citrate, succinate and fumarate were highly abundant in the 3 h samples of b1 (Table S3).

3.3.7. Changes in pathways related to translations

In total, 7 of these 25 genes (*gatB*, *gatC*, *alaS*, *aspS*, *valS*, *ileS* and *lysS*) were mutated (Table S1) in aminoacyl-tRNA biosynthesis pathway. Only *lysS* encoding lysine-tRNA ligase (Ito et al., 1993) was up-regulated at all the sampling points (Table S2). Additionally, the relative content of lysine in b1 was higher than that in b2 at 3 h and 108 h (Table S3).

3.3.8. Changes in pathways related to nucleotide metabolism

Unexpectedly, the mutation rates of genes related to purine (Fig. 5) and pyrimidine metabolism (Fig. 6) were 46% (23/50) and 48% (17/35) after mutagenesis, respectively (Table S1). IMP serves as a central branch point in the pathway of purine metabolism (Pimkin et al., 2009), whereas genes encoding proteins that catalyze the de novo synthesis of IMP from 5-phosphoribosyl 1-pyrophosphate (PRPP) were mostly mutated (including *purN*, *purQ*, *purK*, *purE*, *purC*, *purB* and *purH*)

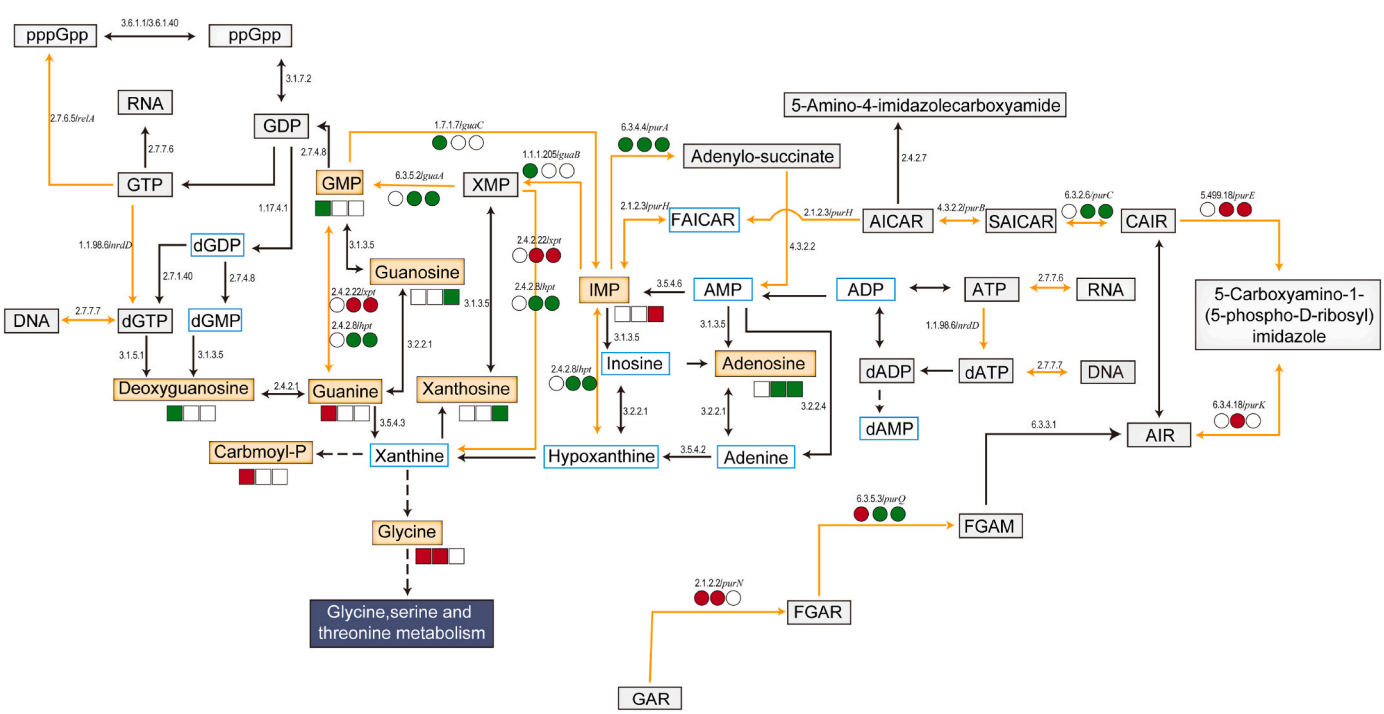

Fig. 5. Multiomics identified differences between acid-tolerant and acid-sensitive *O. oeni* in the purine metabolism pathway during three growth stages when *O. oeni* suffers high AS. Yellow connection lines represented the intragenic SNPs; the color circles represented the gene expression levels with intragenic SNPs (red, up-regulated; green, down-regulated; white, no significant change); the orange box indicated significant differences in metabolites between b1 and b2 mutants; blue frame box were the detected metabolites with no significant differences; color rectangles were the relative content changes of metabolites during three growth stages (red, higher content; green, lower content; white, no significant change). (For interpretation of the references to color in this figure legend, the reader is referred to the Web version of this article.)

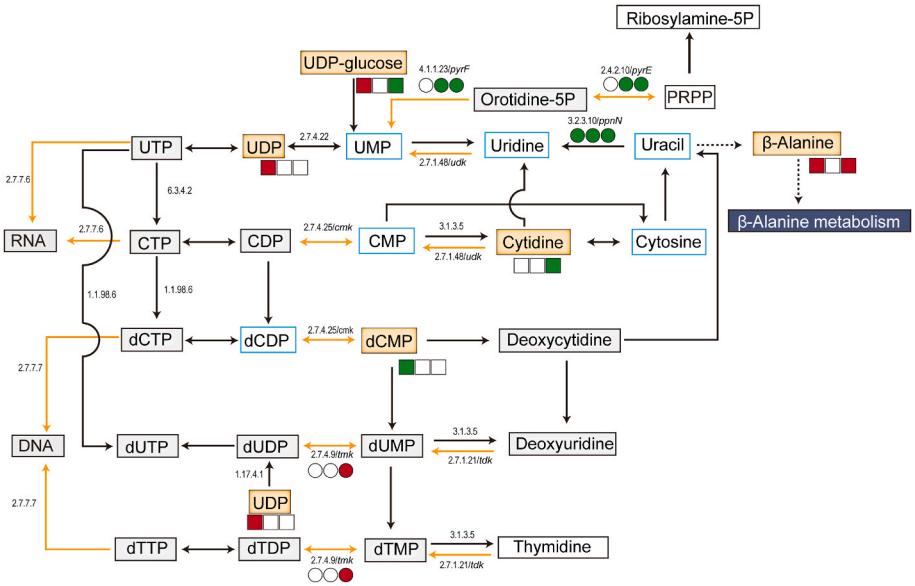

Fig. 6. Multiomics identified differences between acid-tolerant and acid-sensitive *O. oeni* in the pyrimidine metabolism pathway during three growth stages when *O. oeni* suffers high AS. Yellow connection lines represented the intragenic SNPs; the color circles represented the gene expression levels with intragenic SNPs (red, up-regulated; green, down-regulated; white, no significant change); the orange box indicated significant differences in metabolites between b1 and b2 mutants; blue frame box were the detected metabolites with no significant differences; color rectangles were the relative content changes of metabolites during three growth stages (red, higher content; green, lower content; white, no significant change). (For interpretation of the references to color in this figure legend, the reader is referred to the Web version of this article.)

(Warren et al., 1996). Furthermore, the *guaC* gene encoding a protein that can regenerate IMP from GMP was also mutated (Pimkin et al., 2009). Additionally, genes encoding proteins involved in the conversion of IMP into AMP, XMP or GMP, and their deoxygenated forms, which were ultimately utilized for DNA or RNA biosynthesis, also exhibited mutation. Transcriptomic data indicated that *purN* was up-regulated in the 3 h and 36 h samples, and *purE* and *xpt* in the 36 h and 108 h samples, *purK* in the 36 h samples, and the expression levels of others genes were down-regulated and variable at different sampling points (Table S2).

In the pyrimidine metabolic pathway, gene include *udk*, *tdk*, *cmk* and *tmk* were mutated (Table S1). Of them, *udk* can phosphorylate both uridine and cytidine to their monophosphate forms (Valentin-Hansen, 1978). Then, *cmk,* specifically phosphorylates CMP or dCMP using ATP as the favored phosphoryl donor (Bertrand et al., 2002). The *tdk* gene phosphorylates both deoxyuridine and thymidine (Falke et al., 1982), and *tmk* subsequently phosphorylates dUMP or dTMP (Nelson and Carter, 1969). Among these genes, only *tmk* was up-regulated in the 108 h samples (Table S2). Notably, genes encoding for DNA and RNA polymerases also showed mutations (Table S1). Among these mutated genes, *polC*, *dnaE* and *dnaX* encode DNA polymerases; *rpoA*, *rpoB* and *rpoZ* encode RNA polymerases. *polC* expression was down-regulated in the 3 h samples and *dnaX* expression was up-regulated in the 36 h and 108 h samples (Table S2).

3.3.9. Changes related to membrane transporters

A total of 23 genes were mutated in the ABC transporter pathway (Table S1): the gene *metI* is responsible for the uptake of methionine (Merlin et al., 2002); *pstS* and *pstC* are essential for phosphate utilization (Braibant et al., 1996); *ugpE* and *ugpC* are involved in the transport of sn-glycerol-3P (Hekstra and Tommassen, 1993; Overduin et al., 1988); *ecfT*, *ecfA1* and *ecfA2* are responsible for the utilization of biotin (Karpowich and Wang, 2013); *ssuB* and *ssuC* are essential for alkanesulfonate utilization (Eichhorn et al., 2000; Endoh et al., 2003).

Transcriptomic data (Table S2) showed that *ugpC* expression was up-regulated at all the sampling points, and *ugpE* in the 3 h and 36 h samples was up-regulated, as well as *ssuC* in the 3 h and 108 h samples, and *ssuB* in the 36 h and 108 h samples. However, *metI* expression was down-regulated in the 3 h and 36 h samples, *ecfA1* was down-regulated in the 36 h and 108 h samples.

Metabolomics data showed (Table S3) that the metabolites related to above-mentioned genes were not detected at any of the three sampling stages, except for the increased level of biotin in the 3 h samples, which may be due to the rapid metabolism of these intermediate metabolites by the cells.

3.3.10. Changes in pathway related to lipid metabolism

The gene *gpsA* encoding dihydroxyacetone phosphate reductases (a key factor responsible for the synthesis of sn-glycerol-3P) (Morbidoni et al., 1995; Sakasegawa et al., 2004) had been mutated (Fig. 3 and Table S2). Additionally, the relative metabolite contents (including sn-*glycero*-3-phosphocholine, choline, phosphocholine and CDP-choline) in b1 were higher than that in b2 at 3 h (Table S3).

3.3.11. Changes in pathways related to cofactors and vitamins

Genes including *nadK* and *pntA* encode proteins that catalyze the transfer of a hydride ion between nicotinamide adenine dinucleotide (NAD) and oxidized nicotinamide dinucleotide phosphate (NADP) (Zieger and Ware, 1997). *pntA* was down-regulated in the 108 h samples (Table S2). In addition, the relative content of nicotinamide was high at all sampling times, and NAD^+ was high in the 3 h and 108 h samples (Table S3). In the folate biosynthesis pathway, the gene *folA* encoding dihydrofolate reductase which catalyze reversible conversion between THF (5,6,7,8-tetrahydrofolate) and DHF (7,8-dihydrofolate), has been mutated, and it was down-regulated at all the sampling points (Table S2).

4. Discussion

In this study, we employed low-energy N^+ beam implantation combined with stress selection to successfully obtain 6 mutants with significantly different phenotypes and a wide range of genetic mutation and genetic traits. Additionally, the strains b1/b2, a3/a1, and c1/c2 were derived from wild-type *O. oeni* SX-1b, SX-1a, and CS-1b, respectively. The paired mutants from the same wild-type strains have the same genetic background and are therefore ideal candidates for studying AS response.

By comparative genomic, the blue module in WGCNA analysis of transcriptomic and metabolomic analysis, our research revealed the integrated changes to AS in *O. oeni*.

4.1. Cell membrane, the first barrier fighting against AS

Cell membranes, a semipermeable barrier, are essential to control ionic permeability and to regulate solute exchange between *in vivo* and

the external media and act as the first barrier of protection strains against external AS (Bastianini et al., 2000; Da Silveira et al., 2003; Tourdot-Marechal et al., 2000; Yang et al., 2014; Zhang et al., 2013; Zhao et al., 2009). AS leads to cell membrane phospholipid and protein changes; therefore, membrane fluidity likely changes and exerts a rigidifying effect on the cell membrane (Son et al., 2005) which, in turn, may activate signal transduction, inducing stress gene expression (Coucheney et al., 2005).

Our results indicated that the genes associated with ABC transporters and glycerophospholipid metabolism not only exhibited mutation sites but also had different expression levels (Table 1 and Table S2). ABC transporters constitute one of the largest protein families with diverse functions in membrane transport (Bourdineaud et al., 2004; Lorca et al., 2007). Additionally, our results also showed a higher mutation rates (30%, 23/77) in ABC transporters. Whether the mutations alter the conformational equilibrium of related transporter and therefore increase/decrease the efficiency of transport, deserve further investigation. Glycerophospholipid are the main phospholipids constituents of the cell membrane, and they also function as membrane surfactants involved in signaling and protein-protein recognition (Fisette et al., 2016; Fonseca et al., 2019). Metabolomic data also shows that the choline compounds, a synthetic precursor of many phospholipids, are high content in 3 h (Table S3). In addition, fatty acid biosynthesis, fatty acid metabolism, and phosphotransferase system (PTS), showed significant enrichment in both genomic and transcriptomic analysis.

Even though cell membranes exhibit protection against environment stress, AS can still cause a decrease in intracellular pH, which can lead to a series of cellular changes such as enzyme inactivation, the release of DNA purines and pyrimidines, and even genomic damage (van de Guchte et al., 2002).

4.2. Multiple intracellular processes constituting an intricate and interconnected acid regulation network

The vast majority of enriched pathways are subjected to intracellular regulation (Table 1). In addition, the metabolism of carbohydrates and amino acids constitutes the largest proportion, mainly because carbon and nitrogen sources are two essential components for the growth and metabolism of microorganisms (de Nadra et al., 1999). Even though ATB medium was rich in glucose, the relative content of glucose in b1 was only higher than that in b2 at 3 h, whereas lactose in b1 was higher at all the sampling points according to metabolomic data. This possibly due to the fact that *O. oeni* has already adapted to the harsh environment with scarce glucose and fructose after alcoholic fermentation in wine-making (Grandvalet, 2017). And perhaps they have developed their own mechanism on glucose starvation. Thus cells might need to catalyze polysaccharides or disaccharides to monosaccharides and then use the generated monosaccharides as glycosyl donors (Mafa et al., 2020), providing alternative carbon sources, ATP or NADH (Fang et al., 2020; Mun and Chang, 2020).

Notably, glycolysis, pyruvate, and the 2-oxoglutartate-glutamate-glutamine cycle often serve as central metabolic pathways that provide most of the precursors required for the synthesis of cellular macromolecules (Hartmann et al., 2013; Kang et al., 2013; Sonenshein, 2007). Moreover, purine and pyrimidine pathways are essential for many cellular physiological processes. They work as building blocks in DNA and RNA synthesis, are utilized as an energy supplier (ATP) for cellular metabolism, and also play key role in regulatory functions (cAMP, *carB*, etc.) (Garavaglia et al., 2012; Warren et al., 1996). These pathways should be highly conserved because these biochemical pathways are prevalent in the biological world, but each has one or more mutant genes in our experiments. This finding may be able to point to a possible direction for further studies on the evolution trends of acid-tolerant microorganisms.

We also showed that, some amino acid-dependent resistance systems were detected existing changes in all three omics study, which has been reported able to enhance the acid tolerance of bacteria during metabolism (Guan and Liu, 2020; Senouci-Rezkallah et al., 2011), including arginine (Casiano-Colon and Marquis, 1988; Zhao et al., 2019), glutamate (Lu et al., 2013), proline (Di Martino et al., 2020), aspartate (Hu et al., 2010), lysine (He et al., 2017), and valine, leucine and isoleucine (branch amino acid, BCAAs). What's more, in our study, it is very interesting that almost all the above-mentioned amino acids showed higher content in b1 than in b2 at 3 h.

Among the above-mentioned amino acid-dependent acid resistance systems, arginine and glutamate metabolism systems are the earliest discovered and most studied resistance mechanisms against AS (Casiano-Colon and Marquis, 1988; Lu et al., 2013; Margalef-Catala et al., 2016a; Vasserot et al., 2003; Zhao et al., 2019). Besides, arginine can serve as an energy source for glutamate decarboxylation (Laroute et al., 2016), as *O. oeni* does not have an endogenous energy stock, and the transport of glutamate in *O. oeni* is energy dependent. However, it could be compensated by other energetics, such as arginine metabolism or carbohydrates (Vasserot et al., 2003). Aspartate is able to maintain homeostasis in the cytoplasmic pH by releasing ammonia during metabolism (Hu et al., 2010), and it is also an essential precursor for the biosynthesis of some other amino acids (lysine, methionine, threonine and isoleucine) (Curien et al., 2005; Hansen et al., 2009) and pyrimidine (Bechtloff et al., 1999; Burns et al., 1998; Zhang et al., 2017). Aspartate can also be converted to orotidine-5P (Fig. 3), and orotidine-5P can be further converted into PRPP, an important precursor in the nucleotide synthetic pathways, which makes aspartate an important role in salvage synthesis of nucleotide (Becerra and Lazcano, 1998; Donini et al., 2017; Hansen et al., 2014). Remarkably, our research revealed that striking mutations occurred in the 4 genes encoding proteins that catalyze aspartate into orotidine-5P (Fig. 3). Also, 3 of these genes were significantly down-regulated in b1 at 36 h and 108 h (Table S2). Therefore, the roles of nucleotide salvage synthesis through aspartate metabolism on acid regulation deserve further exploration and study.

Furthermore, we had enriched cysteine, methionine, glutathione, glycine, serine and threonine related metabolic pathways (Table 1), which suggested that the changes in these pathways may also participate in acid regulation. Among them, methionine is the main precursor of glutathione and cysteine, in addition to being the precursor of S-adenosylmethionine (SAM), the main donor of the methyl group and a central molecule in one-carbon metabolism (Alehagen et al., 2019; Auger et al., 2002), and we already mentioned that gene *metI* encording methionine transporter was mutated in the genomic research. GSH as an important source of sulfhydryl groups in the majority of living cells, plays an important role in maintaining the proper redox state of sulfhydryl groups in proteins, which is beneficial to the enzyme reaction and could increase stress tolerance in bacteria (Margalef-Catala et al., 2017; Margalef-Catala et al., 2016b; Zhao et al., 2019). For instance, Zhang et al. (2007) reported that added GSH significantly increased the activity of glyceraldehyde-3-phosphate dehydrogenase of *Lactococcus lactis* under oxidative stress.

Further studies are also needed in the integrated pathways include folate biosynthesis, sulfur metabolism, nicotinate and nicotinamide metabolism. Tetrahydrofolate (THF), the reduced form of folic acid, functions as the donor of one-carbon units in numerous metabolic pathways is involved in the biosynthesis of purine, thymidine, glycine and methionine (Bermingham and Derrick, 2002; Giladi et al., 2003; Kwon et al., 2010). Sulfur metabolism has been already reported to be involved in *Acidithiobacillus acldus* acid regulation (pH 1.1) (Mangold et al., 2013). We hypothesized that nicotinate and nicotinamide metabolism might be closely related to acid regulation through changing intracellular redox state (Fig. 4).

4.3. Transcriptomic and metabolomic data demonstrating dynamic changes in cells at different growth stages

Transcriptomic and metabolomic data showed that different survival

and proliferation response existed at different phases under AS. The highest number of DEGs was observed in the 108 h samples, the highest number of differential metabolites in the 3 h samples, and the smallest changes in both DEGs and differential metabolites in the 36 h samples. The possible reason for these phenomena may be that different stages of *O. oeni* have different acid response strategies.

5. Conclusions

Genomic, transcriptomic and metabolomic data revealed great differences between acid-tolerant *O. oeni* mutant and acid-sensitive *O. oeni* mutant. Moreover, the integrative analysis showed that the ability of the strain to tolerate AS was regulated by the interaction of multiple mechanisms, and also the mechanisms changed at different growth stages. These findings could give new insights to further study molecular mechanisms response to AS in LAB, which could provide specific strategies for breed and improvement of LAB adapted to high AS, as well as for the optimization of fermentation process under high AS.

Declaration of competing interest

The author declared no conflicts of interest.

Acknowledgments

We are very grateful to members of Shuwen Liu's lab for discussions and comments.

Appendix A. Supplementary data

Supplementary data to this article can be found online at https://doi.org/10.1016/j.fm.2021.103905.

Authors' contributions

Supervisors: S L. and K S. Experiments: Q C. and X Y. Figures: Q C., X Y. and Q M. Data analysis: Q C., X Y., L Z., L H. and Y Y. Manuscript: Q C., X Y. and K S. Data submissions: Q C., X Y. and W C.

Funding

This work was financially supported by the National Natural Science Foundation of China (32072206), the National Key R&D Program of China (2019YFD1002503) and the China Technology Agriculture Research System (CARS-29-jg-3).

Declarations

Ethics approval and consent to participate.
No applicable.

Consent for publication

All authors have read and agreed with the manuscript.

Availability of data and materials

All raw and processed sequencing data generated in this study have been submitted to the NCBI Sequence Read Archive (SRA; https://submit.ncbi.nlm.nih.gov/) under accession numbers SAMN17084025, SAMN17084026, SAMN17084027, SAMN17084028, SAMN17084029, SAMN17084030, SAMN17084031, SAMN17084032, SAMN17084033, SAMN17084034, SAMN17084035, SAMN17084036, SAMN17084037, SAMN17084038, SAMN17084039, SAMN17084040, SAMN17084041, SAMN17084042; SAMN05000093, SAMN05000094, SAMN05000095, SAMN05000096, SAMN05000097 and SAMN05000098.

References

Alehagen, U., Johansson, P., Aaseth, J., Alexander, J., Surowiec, I., Lundstedt-Enkel, K., Lundstedt, T., 2019. Significant changes in metabolic profiles after intervention with selenium and coenzyme Q10 in an elderly population. Biomolecules 9. https://doi.org/10.3390/biom9100553.

Auger, S., Yuen, W.H., Danchin, A., Martin-Verstraete, I., 2002. The *metIC* operon involved in methionine biosynthesis in *Bacillus subtilis* is controlled by transcription antitermination. Microbiology-Sgm 148, 507–518. https://doi.org/10.1099/00221287-148-2-507.

Ai, D.M., Wang, Y.D., Li, X.X., Pan, H.F., 2020. Colorectal cancer prediction based on weighted gene co-expression network analysis and variational auto-encoder. Biomolecules 10. https://doi.org/10.3390/biom10091207.

Bartsch, K., von Johnn-Marteville, A., Schulz, A., 1990. Molecular analysis of two genes of the *Escherichia coli gab* cluster: nucleotide sequence of the glutamate:succinic semialdehyde transaminase gene (*gabT*) and characterization of the succinic semialdehyde dehydrogenase gene (*gabD*). J. Bacteriol. 172, 7035–7042. https://doi.org/10.1039/c4an01352b.

Bastianini, A., Granchi, L., Guerrini, S., Vincenzini, M., 2000. Fatty acid composition of malolactic *Oenococcus oeni* strains exposed to pH and ethanol stress. Ital. J. Food Sci. 12, 333–342. https://doi.org/10.1080/096374800100868.

Becerra, A., Lazcano, A., 1998. The role of gene duplication in the evolution of purine nucleotide salvage pathways. Orig. Life Evol. Biosph. 28, 539–553. https://doi.org/10.1023/A:1006500327962.

Bechtloff, D., Grunenfelder, B., Akerlund, T., Nordstrom, K., 1999. Analysis of protein synthesis rates after initiation of chromosome replication in *Escherichia coli*. J. Bacteriol. 181, 6292–6299. https://doi.org/10.1557/PROC-504-135.

Bermingham, A., Derrick, J.P., 2002. The folic acid biosynthesis pathway in bacteria: evaluation of potential for antibacterial drug discovery. Bioessays 24, 637–648. https://doi.org/10.1002/bies.10114.

Bertrand, T., Briozzo, P., Assairi, L., Ofiteru, A., Bucurenci, N., Munier-Lehmann, H., Golinelli-Pimpaneau, B., Barzu, O., Gilles, A.M., 2002. Sugar specificity of bacterial CMP kinases as revealed by crystal structures and mutagenesis of *Escherichia coli* enzyme. J. Mol. Biol. 315, 1099–1110. https://doi.org/10.1006/jmbi.2001.5286.

Bilder, P., Lightle, S., Bainbridge, G., Ohren, J., Finzel, B., Sun, F., Holley, S., Al-Kassim, L., Spessard, C., Melnick, M., Newcomer, M., Waldrop, G.L., 2006. The structure of the carboxyltransferase component of acetyl-CoA carboxylase reveals a zinc-binding motif unique to the bacterial enzyme. Biochemistry 45, 1712–1722. https://doi.org/10.1021/bi0520479.

Bourdineaud, J.P., Nehme, B., Tesse, S., Lonvaud-Funel, A., 2004. A bacterial gene homologous to ABC transporters protect *Oenococcus oeni* from ethanol and other stress factors in wine. Int. J. Food Microbiol. 92, 1–14. https://doi.org/10.1016/S0168-1605(03)00162-4.

Braibant, M., Lefevre, P., de Wit, L., Ooms, J., Peirs, P., Huygen, K., Wattiez, R., Content, J., 1996. Identification of a second *Mycobacterium tuberculosis* gene cluster encoding proteins of an ABC phosphate transporter. FEBS Lett. 394, 206–212. https://doi.org/10.1016/0014-5793(96)00953-2.

Budin-Verneuil, A., Maguin, E., Auffray, Y., Ehrlich, D.S., Pichereau, V., 2006. Genetic structure and transcriptional analysis of the arginine deiminase (ADI) cluster in *Lactococcus lactis* MG1363. Can. J. Microbiol. 52, 617–622. https://doi.org/10.1139/w06-009.

Burns, B.P., Mendz, G.L., Hazell, S.L., 1998. A novel mechanism for resistance to the antimetabolite N-phosphonoacetyl-L-aspartate by *Helicobacter pylori*. J. Bacteriol. 180, 5574–5579. https://doi.org/10.1016/S0016-5107(98)70203-2.

Casiano-Colon, A., Marquis, R.E., 1988. Role of the arginine deiminase system in protecting oral bacteria and an enzymatic basis for acid tolerance. Appl. Environ. Microbiol. 54, 1318–1324. https://doi.org/10.1128/AEM.54.6.1318-1324.1988.

Cheng, C.Y., Chen, J.S., Shan, Y., Fang, C., Liu, Y., Xia, Y., Song, H.H., Fang, W.H., 2013. *Listeria monocytogenes* ArcA contributes to acid tolerance. J. Med. Microbiol. 62, 813–821. https://doi.org/10.1099/jmm.0.055145-0.

Coucheney, F., Gal, L., Beney, L., Lherminier, J., Gervais, P., Guzzo, J., 2005. A small HSP, Lo18, interacts with the cell membrane and modulates lipid physical state under heat shock conditions in a lactic acid bacterium. Biochim. Biophys. Acta Biomembr. 1720, 92–98. https://doi.org/10.1016/j.bbamem.2005.11.017.

Curien, G., Ravanel, S., Robert, M., Dumas, R., 2005. Identification of six novel allosteric effectors of *Arabidopsis thaliana* aspartate kinase-homoserine dehydrogenase isoforms - physiological context sets the specificity. J. Biol. Chem. 280, 41178–41183. https://doi.org/10.1074/jbc.M509324200.

Da Silveira, M.G., Golovina, E.A., Hoekstra, F.A., Rombouts, F.M., Abee, T., 2003. Membrane fluidity adjustments in ethanol-stressed *Oenococcus oeni* cells. Appl. Environ. Microbiol. 69, 5826–5832. https://doi.org/10.1128/AEM.69.10.5826-5832.2003.

Davis, C.R., Wibowo, D.J., Lee, T.H., Fleet, G.H., 1986. Growth and metabolism of lactic acid bacteria during and after malolactic fermentation of wines at different pH. Appl. Environ. Microbiol. 51, 539–545. https://doi.org/10.1016/S0769-2609(86)80024-2.

de Nadra, M.C. Manca, Farias, M.E., Moreno-Arribas, V., Pueyo, E., Polo, M.C., 1999. A proteolytic effect of*Oenococcus oeni*on the nitrogenous macromolecular fraction of red wine. Fems Microbiol. Lett. 174 (1), 41–47. https://doi.org/10.1111/j.1574-6968.1999.tb13547.x.

Di Martino, C., Testa, B., Letizia, F., Iorizzo, M, Lombardi, S.J., Ianiro, M., Di Renzo, M., Strollo, D., Coppola, R., 2020. Effect of exogenous proline on the ethanolic tolerance

and malolactic performance of *Oenococcus oeni*. J. Food Sci. Technol. Mysore 57 (11), 3973–3979. https://doi.org/10.1007/s13197-020-04426-1.

Donini, S., Ferraris, D.M., Miggiano, R., Massarotti, A., Rizzi, M., 2017. Structural investigations on orotate phosphoribosyltransferase from *Mycobacterium tuberculosis*, a key enzyme of the de novo pyrimidine biosynthesis. Sci. Rep. 7 https://doi.org/10.1038/s41598-017-01057-z.

Eichhorn, E., van der Ploeg, J.R., Leisinger, T., 2000. Deletion analysis of the *Escherichia coli* taurine and alkanesulfonate transport systems. J. Bacteriol. 182, 2687–2695. https://doi.org/10.1128/Jb.182.10.2687-2695.2000.

Endoh, T., Kasuga, K., Horinouchi, M., Yoshida, T., Habe, H., Nojiri, H., Omori, T., 2003. Characterization and identification of genes essential for dimethyl sulfide utilization in *Pseudomonas putida* strain DS1. Appl. Microbiol. Biotechnol. 62, 83–91. https://doi.org/10.1007/s00253-003-1233-7.

Falke, D., Labenz, J., Brauer, D., Muller, W.E., 1982. Adenosine diphosphate: thymidine 5'-phosphotransferase, a new enzyme activity, associated with the Herpes simplex virus-induced deoxypyrimidine kinase. Biochim. Biophys. Acta 708, 99–103. https://doi.org/10.1016/0167-4838(82)90207-2.

Fang, C., Fang, X.W., Chen, X.Y., Wang, C., Liang, X.Y., Gu, Y.F., Fang, W.H., Yang, Y.Y., 2020. Evaluating the contribution of acid resistance Systems and probing the different roles of the glutamate decarboxylases of *Listeria monocytogenes* under acidic conditions. Kafkas Universitesi Veteriner Fakultesi Dergisi 26, 231–238. https://doi.org/10.9775/kvfd.2019.22784.

Fisette, O., Paslack, C., Barnes, R., Isas, J.M., Langen, R., Heyden, M., Han, S., Schafer, L. V., 2016. Hydration dynamics of a peripheral membrane protein. J. Am. Chem. Soc. 138, 11526–11535. https://doi.org/10.1021/jacs.6b07005.

Fonseca, F., Penicaud, C., Tymczyszyn, E.E., Gomez-Zavaglia, A., Passot, S., 2019. Factors influencing the membrane fluidity and the impact on production of lactic acid bacteria starters. Appl. Microbiol. Biotechnol. 103, 6867–6883. https://doi.org/10.1007/s00253-019-10002-1.

Fortier, L.C., Tourdot-Marechal, R., Divies, C., Lee, B.H., Guzzo, J., 2003. Induction of *Oenococcus oeni* H^+-ATPase activity and mRNA transcription under acidic conditions. FEMS Microbiol. Lett. 222, 165–169. https://doi.org/10.1016/S0378-1097(03)00299-4.

Fries, M., Jung, H.I., Perham, R.N., 2003. Reaction mechanism of the heterotetrameric (alpha2beta2) E1 component of 2-oxo acid dehydrogenase multienzyme complexes. Biochemistry 42, 6996–7002. https://doi.org/10.1021/bi027397z.

Garavaglia, M., Rossi, E., Landini, P., 2012. The pyrimidine nucleotide biosynthetic pathway modulates production of biofilm determinants in *Escherichia coli*. PloS One 7, e31252. https://doi.org/10.1371/journal.pone.0031252.

Garcia-Diez, J., Saraiva, C., 2021. Use ofstarter cultures in foods from animal origin to improve their safety. Int. J. Environ. Res. Publ. Health 18. https://doi.org/10.3390/ijerph18052544.

Giladi, M., Altman-Price, N., Levin, I., Levy, L., Mevarech, M., 2003. FolM, a new chromosomally encoded dihydrofolate reductase in *Escherichia coli*. J. Bacteriol. 185, 7015–7018. https://doi.org/10.1128/jb.185.23.7015-7018.2003.

Guan, N.Z., Liu, L., 2020. Microbial response to acid stress: mechanisms and applications. Appl. Microbiol. Biotechnol. 104, 51–65. https://doi.org/10.1007/s00253-019-10226-1.

Guzzon, R., Poznanski, E., Conterno, L., Vagnoli, P., Krieger-Weber, S., Cavazza, A., 2009. Selection of a new highly resistant strain for malolactic fermentation under difficult conditions. South Afr. J. Enol. Vitic. 30, 133–141. https://doi.org/10.1016/j.postharvbio.2008.06.006.

Grandvalet, C., 2017. *Oenococcus oeni*: queen of the cellar, nightmare of geneticists. Microbiol-Sgm 163, 297–299. https://doi.org/10.1099/mic.0.000456.

Hansen, M., Friis, C., Bowra, S., Holm, P.B., Vincze, E., 2009. A pathway-specific microarray analysis highlights the complex and co-ordinated transcriptional networks of the developing grain of field-grown barley. J. Exp. Bot. 60, 153–167. https://doi.org/10.1093/jxb/ern270.

Hansen, M.R., Barr, E.W., Jensen, K.F., Willemoes, M., Grubmeyer, C., Winther, J.R., 2014. Catalytic site interactions in yeast OMP synthase. Arch. Biochem. Biophys. 542, 28–38. https://doi.org/10.1016/j.abb.2013.11.004.

Hartmann, T., Zhang, B., Baronian, G., Schulthess, B., Homerova, D., Grubmuller, S., Kutzner, E., Gaupp, R., Bertram, R., Powers, R., Eisenreich, W., Kormanec, J., Herrmann, M., Molle, V., Somerville, G.A., Bischoff, M., 2013. Catabolite control protein E (CcpE) is a LysR-type transcriptional regulator of tricarboxylic acid cycle activity in *Staphylococcus aureus*. J. Biol. Chem. 288, 36116–36128. https://doi.org/10.1074/jbc.M113.516302.

He, A., Penix, S.R., Basting, P.J., Griffith, J.M., Creamer, K.E., Camperchioli, D., Clark, M. W., Gonzales, A.S., Erazo, J.S.C., George, N.S., Bhagwat, A.A., Slonczewski, J.L., 2017. Acid evolution of *Escherichia coli* K-12 eliminates amino acid decarboxylases and reregulates catabolism. Appl. Environ. Microbiol. 83 https://doi.org/10.1128/AEM.00442-17.

Hekstra, D., Tommassen, J., 1993. Functional exchangeability of the ABC proteins of the periplasmic binding protein-dependent transport systems Ugp and Mal of *Escherichia coli*. J. Bacteriol. 175, 6546–6552. https://doi.org/10.1128/jb.175.20.6546-6552.1993.

Hu, Y.B., Lu, P., Zhang, Y., Li, L.M., Chen, S.Y., 2010. Characterization of an aspartate-dependent acid survival system in *Yersinia pseudotuberculosis*. FEBS Lett. 584, 2311–2314. https://doi.org/10.1016/j.febslet.2010.03.045.

Ito, K., Kawakami, K., Nakamura, Y., 1993. Multiple control of *Escherichia-coli* lysyl-transfer rna-synthetase expression involves a transcriptional repressor and a translational enhancer element. Proceedings of the National Academy of Sciences USA 90, 302–306. https://doi.org/10.1073/pnas.90.1.302.

Ji, M., Barnwell, C.V., Grunden, A.M., 2015. Characterization of recombinant glutathione reductase from the psychrophilic Antarctic bacterium *Colwellia psychrerythraea*. Extremophiles 19, 863–874. https://doi.org/10.1007/s00792-015-0762-1.

Jin, G., Wang, H., Zhang, C.H., Li, C.X., Du, L.Y., Grbin, P.R., Li, H., 2014. Characterization and amino acid metabolism performances of indigenous *Oenococcus oeni* isolated from Chinese wines. Eur. Food Res. Technol. 238, 597–605. https://doi.org/10.1007/s00217-013-2112-9.

Kang, T.S., Korber, D.R., Tanaka, T., 2013. Contributions of citrate in redox potential maintenance and ATP production: metabolic pathways and their regulation in *Lactobacillus panis* PM1. Appl. Microbiol. Biotechnol. 97, 8693–8703. https://doi.org/10.1007/s00253-013-5108-2.

Karpowich, N.K., Wang, D.N., 2013. Assembly and mechanism of a group II ECF transporter. Proc. Natl. Acad. Sci. U. S. A. 110, 2534–2539. https://doi.org/10.1073/pnas.1217361110.

Kwon, Y.K., Higgins, M.B., Rabinowitz, J.D., 2010. Antifolate-induced depletion of intracellular glycine and purines inhibits thymineless death in *E. coli*. ACS Chem. Biol. 5, 787–795. https://doi.org/10.1021/cb100096f.

Laroute, V., Yasaro, C., Narin, W., Mazzoli, R., Pessione, E., Cocaign-Bousquet, M., Loubiere, P., 2016. GABA production in *Lactococcus lactis* is enhanced by arginine and co-addition of malate. Front. Microbiol. 7 https://doi.org/10.3389/fmicb.2016.01050.

Li, Q., Ganzle, M.G., 2020. Host-adapted *lactobacilli* in food fermentations: impact of metabolic traits of host adapted *lactobacilli* on food quality and human health. Curr. Opin. Food Sci. 31, 71–80. https://doi.org/10.1016/j.cofs.2020.02.002.

Liu, Y.L., Li, H., 2009. Integrated expression of the *Oenococcus oeni mleA* gene in *Saccharomyces cerevisiae*. Agric. Sci. China 8, 821–827. https://doi.org/10.1016/S1671-2927(08)60283-7.

Lorca, G.L., Barabote, R.D., Zlotopolski, V., Tran, C., Winnen, B., Hvorup, R.N., Stonestrom, A.J., Nguyen, E., Huang, L.W., Kim, D.S., Saier, M.H., 2007. Transport capabilities of eleven gram-positive bacteria: comparative genomic analyses. Biochim. Biophys. Acta Biomembr. 1768, 1342–1366. https://doi.org/10.1016/j.bbamem.2007.02.007.

Lu, P.L., Ma, D., Chen, Y.L., Guo, Y.Y., Chen, G.Q., Deng, H.T., Shi, Y.G., 2013. L-glutamine provides acid resistance for *Escherichia coli* through enzymatic release of ammonia. Cell Res. 23, 635–644. https://doi.org/10.1038/cr.2013.13.

Mafa, M.S., Dirr, H.W., Malgas, S., Krause, R.W.M., Rashamuse, K., Pletschke, B.I., 2020. A novel dimeric exoglucanase (GH5_38): biochemical and structural characterisation towards its application in alkyl cellobioside synthesis. Molecules 25. https://doi.org/10.3390/molecules25030746.

Mangold, S., Jonna, V.R., Dopson, M., 2013. Response of *Acidithiobacillus caldus* toward suboptimal pH conditions. Extremophiles 17, 689–696. https://doi.org/10.1007/s00792-013-0553-5.

Margalef-Catala, M., Araque, I., Bordons, A., Reguant, C., 2017. Genetic and transcriptional study of glutathione metabolism in *Oenococcus oeni*. Int. J. Food Microbiol. 242, 61–69. https://doi.org/10.1016/j.ijfoodmicro.2016.11.013.

Margalef-Catala, M., Araque, I., Bordons, A., Reguant, C., Bautista-Gallego, J., 2016a. Transcriptomic and proteomic analysis of *Oenococcus oeni* adaptation to wine stress conditions. Front. Microbiol. 7 https://doi.org/10.3389/fmicb.2016.01554.

Margalef-Catala, M., Araque, I., Weidmann, S., Guzzo, J., Bordons, A., Reguant, C., 2016b. Protective role of glutathione addition against wine-related stress in *Oenococcus oeni*. Food Res. Int. 90, 8–15. https://doi.org/10.1016/j.foodres.2016.10.006.

Merlin, C., Gardiner, G., Durand, S., Masters, M., 2002. The *Escherichia coli metD* locus encodes an ABC transporter which includes Abc (MetN), YaeE (MetI), and YaeC (MetQ). J. Bacteriol. 184, 5513–5517. https://doi.org/10.1128/jb.184.19.5513-5517.2002.

Morbidoni, H.R., Demendoza, D., Cronan, J.E., 1995. Synthesis of sn-glycerol 3-phosphate, a key precursor of membrane-lipids, in *Bacillus-Subtilis*. J. Bacteriol. 177, 5899–5905. https://doi.org/10.1128/jb.177.20.5899-5905.1995.

Mun, S.Y., Chang, H.C., 2020. Characterization of *Weissella koreensis* SK isolated from Kimchi fermented at low temperature (around 0 degrees C) based on complete genome sequence and corresponding phenotype. Microorganisms 8. https://doi.org/10.3390/microorganisms8081147.

Murahari, E.C., West, T.P., 2019. The pyrimidine biosynthetic pathway and its regulation in *Pseudomonas jessenii*. Antonie Van Leeuwenhoek International Journal of General and Molecular Microbiology 112, 461–469. https://doi.org/10.1007/s10482-018-1168-8.

Nelson, D.J., Carter, C.E., 1969. Purification and characterization of Thymidine 5-monophosphate kinase from *Escherichia coli* B. J. Biol. Chem. 244, 5254–5262. https://doi.org/10.1002/ajpa.21340.

Norager, S., Arent, S., Bjornberg, O., Ottosen, M., Lo Leggio, L., Jensen, K.F., Larsen, S., 2003. *Lactococcus lactis* dihydroorotate dehydrogenase A mutants reveal important facets of the enzymatic function. J. Biol. Chem. 278, 28812–28822. https://doi.org/10.1074/jbc.M303767200.

Olguin, N., Bordons, A., Reguant, C., 2009. Influence of ethanol and pH on the gene expression of the citrate pathway in *Oenococcus oeni*. Food Microbiol. 26, 197–203. https://doi.org/10.1016/j.fm.2008.09.004.

Overduin, P., Boos, W., Tommassen, J., 1988. Nucleotide sequence of the *ugp* genes of *Escherichia coli* K-12: homology to the maltose system. Mol. Microbiol. 2, 767–775. https://doi.org/10.1111/j.1365-2958.1988.tb00088.x.

Pimkin, M., Pimkina, J., Markham, G.D., 2009. A regulatory role of the bateman domain of IMP dehydrogenase in adenylate nucleotide biosynthesis. J. Biol. Chem. 284, 7960–7969. https://doi.org/10.1074/jbc.M808541200.

Renouf, V., Delaherche, A., Claisse, O., Lonvaud-Funel, A., 2008. Correlation between indigenous *Oenococcus oeni* strain resistance and the presence of genetic markers. J. Ind. Microbiol. Biotechnol. 35, 27–33. https://doi.org/10.1007/s10295-007-0262-0.

Sakasegawa, S.I., Hagemeier, C.H., Thauer, R.K., Essen, L.O., Shima, S., 2004. Structural and functional analysis of the *gpsA* gene product of *Archaeoglobus fulgidus*: a glycerol-3-phosphate dehydrogenase with an unusual NADP(+) preference. Protein Sci. 13, 3161–3171. https://doi.org/10.1110/ps.04980304.

Schurig, H., Beaucamp, N., Ostendorp, R., Jaenicke, R., Adler, E., Knowles, J.R., 1995. Phosphoglycerate kinase and triosephosphate isomerase from the hyperthermophilic bacterium *Thermotoga maritima* form a covalent bifunctional enzyme complex. EMBO J. 14, 442–451. https://doi.org/10.1111/j.1574-6968.1995.tb07792.x.

Senouci-Rezkallah, K., Schmitt, P., Jobin, M.P., 2011. Amino acids improve acid tolerance and internal pH maintenance in *Bacillus cereus* ATCC14579 strain. Food Microbiol. 28, 364–372. https://doi.org/10.1016/j.fm.2010.09.003.

Sikanyika, M., Aragao, D., McDevitt, C.A., Maher, M.J., 2019. The structure and activity of the glutathione reductase from *Streptococcus pneumoniae*. Acta Crystallographica Section F-Structural Biology Communications 75, 54–61. https://doi.org/10.1107/S2053230X18016527.

Son, C.K., Tourdot-Marechal, R., Marechal, P.A., Guzzo, J., 2005. Combined, cold, acid, ethanol shocks in *Oenococcus oeni*: effects on membrane fluidity and cell viability. Biochim. Biophys. Acta Biomembr. 1717, 118–124. https://doi.org/10.1016/j.bbamem.2005.09.015.

Sonenshein, A.L., 2007. Control of key metabolic intersections in *Bacillus subtilis*. Nat. Rev. Microbiol. 5, 917–927. https://doi.org/10.1038/nrmicro1772.

Sugio, T., Matsugi, S., Tanaka, T., Fujita, M., Tano, T., 1995. Purification and some properties of glutathione-reductase from iron-oxidizing bacterium *Thiobacillus-Ferrooxidans*. Biosc. Biotech. Biochem. 59, 1568–1570. https://doi.org/10.1271/bbb.59.1568.

Thoden, J.B., Huang, X.Y., Raushel, F.M., Holden, H.M., 2002. Carbamoyl-phosphate synthetase - creation of an escape route for ammonia. J. Biol. Chem. 277, 39722–39727. https://doi.org/10.1074/jbc.M206915200.

Tian, J., Bryk, R., Shi, S., Erdjument-Bromage, H., Tempst, P., Nathan, C., 2005. *Mycobacterium tuberculosis* appears to lack alpha-ketoglutarate dehydrogenase and encodes pyruvate dehydrogenase in widely separated genes. Mol. Microbiol. 57, 859–868. https://doi.org/10.1111/j.1365-2958.2005.04741.x.

Torriani, S., Felis, G.E., Fracchetti, F., 2011. Selection criteria and tools for malolactic starters development: an update. Ann. Microbiol. 61, 33–39. https://doi.org/10.1007/s13213-010-0072-x.

Tourdot-Marechal, R., Gaboriau, D., Beney, L., Divies, C., 2000. Membrane fluidity of stressed cells of *Oenococcus oeni*. Int. J. Food Microbiol. 55, 269–273. https://doi.org/10.1016/S0168-1605(00)00202-6.

Tsai, M., Koo, J., Yip, P., Colman, R.F., Segal, M.L., Howell, L., 2007. Substrate and product complexes of *Escherichia coli* adenylosuccinate lyase provide new insights into the enzymatic mechanism. J. Mol. Biol. 370, 541–554. https://doi.org/10.1016/j.jmb.2007.04.052.

Valentin-Hansen, P., 1978. Uridine-cytidine kinase from *Escherichia coli*. Methods Enzymol. 51, 308–314. https://doi.org/10.1016/s0076-6879(78)51041-0.

van de Guchte, M., Serror, P., Chervaux, C., Smokvina, T., Ehrlich, S.D., Maguin, E., 2002. Stress responses in lactic acid bacteria. Antonie Van Leeuwenhoek International Journal of General and Molecular Microbiology 82, 187–216. https://doi.org/10.1023/A:1020631532202.

Vasserot, Y., Dion, C., Bonnet, E., Tabary, I., Maujean, A., Jeandet, P., 2003. Transport of glutamate in *Oenococcus oeni* 8403. Int. J. Food Microbiol. 85, 307–311. https://doi.org/10.1016/S0168-1605(02)00541-X.

Versari, A., Parpinello, G.P., Cattaneo, M., 1999. *Leuconostoc oenos* and malolactic fermentation in wine: a review. J. Ind. Microbiol. Biotechnol. 23, 447–455. https://doi.org/10.1038/sj.jim.2900733.

Vigentini, I., Praz, A., Domeneghetti, D., Zenato, S., Picozzi, C., Barmaz, A., Foschino, R., 2016. Characterization of malolactic bacteria isolated from Aosta Valley wines and evidence of psychrotrophy in some strains. J. Appl. Microbiol. 120, 934–945. https://doi.org/10.1111/jam.13080.

Virdis, C., Sumby, K., Bartowsky, E., Jiranek, V., 2021. Lactic acid bacteria in wine: technological advances and evaluation of their functional role. Front. Microbiol. 11 https://doi.org/10.3389/fmicb.2020.612118.

Wang, W.Y., Gorrell, A., Honzatko, R.B., Fromm, H.J., 1997. A study of *Escherichia coli* adenylosuccinate synthetase association states and the interface residues of the homodimer. J. Biol. Chem. 272, 7078–7084. https://doi.org/10.1074/jbc.272.11.7078.

Warren, M.S., Mattia, K.M., Marolewski, A.E., Bankovic, S.J., 1996. The transformylase enzymes of de novo purine biosynthesis. Pure Appl. Chem. 68, 2029–2036. https://doi.org/10.1351/pac199668112029.

Yamaguchi, M., 1979. Studies on regulatory functions of malic enzymes. IV. Effects of sulfhydryl group modification on the catalytic function of NAD-linked malic enzyme from *Escherichia coli*. J. Biochem. 86, 325–333. https://doi.org/10.1093/oxfordjournals.jbchem.a132530.

Yang, Y.S., Kadim, M.I., Khoo, W.J., Zheng, Q.W., Setyawati, M.I., Shin, Y.J., Lee, S.C., Yuk, H.G., 2014. Membrane lipid composition and stress/virulence related gene expression of *Salmonella Enteritidis* cells adapted to lactic acid and trisodium phosphate and their resistance to lethal heat and acid stress. Int. J. Food Microbiol. 191, 24–31. https://doi.org/10.1016/j.ijfoodmicro.2014.08.034.

Zhang, B.X., Tornmalm, J., Widengren, J., Vakifahmetoglu-Norberg, H., Norberg, E., 2017. Characterization of the role of the malate dehydrogenases to lung tumor cell survival. J. Canc. 8, 2088–2096. https://doi.org/10.7150/jca.19373.

Zhang, G.Q., Fan, M.T., Lv, Q., Li, Y.H., Liu, Y.L., Zhang, S.F., Zhang, H., 2013. The effect of cold, acid and ethanol shocks on synthesis of membrane fatty acid, freeze-drying survival and malolactic activity of *Oenococcus oeni*. Ann. Microbiol. 63, 477–485. https://doi.org/10.1007/s13213-012-0492-x.

Zhang, J., Fu, R.Y., Hugenholtz, J., Li, Y., Chen, J., 2007. Glutathione protects *Lactococcus lactis* against acid stress. Appl. Environ. Microbiol. 73, 5268–5275. https://doi.org/10.1128/AEM.02787-06.

Zhao, H., Yuan, L., Hu, K., Liu, L., Peng, S., Li, H., Wang, H., 2019. Heterologous expression of *ctsR* from *Oenococcus oeni* enhances the acid-ethanol resistance of *Lactobacillus plantarum*. FEMS Microbiol. Lett. 366 https://doi.org/10.1093/femsle/fnz192.

Zhao, H.Y., Liu, L.X., Peng, S., Yuan, L., Li, H., Wang, H., 2019. Heterologous expression of argininosuccinate synthase from *Oenococcus oeni* enhances the acid resistance of *Lactobacillus plantarum*. Front. Microbiol. 10 https://doi.org/10.3389/fmicb.2019.01393.

Zhao, W.Y., Li, H., Wang, H., Li, Z.C., Wang, A.L., 2009. The effect of acid stress treatment on viability and membrane fatty acid composition of *Oenococcus oeni* SD-2a. Agric. Sci. China 8, 311–316. https://doi.org/10.1016/S1671-2927(08)60214-X.

Zieger, B., Ware, J., 1997. Cloning and deduced amino acid sequence of human nicotinamide nucleotide transhydrogenase. DNA Seq 7, 369–373. https://doi.org/10.3109/10425179709034058.